

Planetary interiors:
Magnetic fields, Convection and Dynamo Theory
4. Core dynamics: Rotation and Magnetic fields

Chris Jones, Department of Applied Mathematics
University of Leeds UK

FDEPS Lecture 4, Kyoto, 30th November 2017

Section 4.

Core dynamics: Rotation and Magnetic fields

4.1 Rotating magnetoconvection

We have seen how magnetic fields can be created by dynamo action, but how do they affect the fluid flow?

A region of fluid in which there is a current density \mathbf{j} flowing in a magnetic field \mathbf{B} experiences a body force $\mathbf{j} \times \mathbf{B}$. This force is called the Lorentz force. It arises because electrons and ions moving in a magnetic field experience a force.

The Navier-Stokes equation in a rotating frame then becomes

$$\frac{\partial \mathbf{u}}{\partial t} + 2\Omega \hat{\mathbf{z}} \times \mathbf{u} = -\frac{1}{\rho} \nabla p + g\alpha T' \hat{\mathbf{z}} + \frac{1}{\rho} \mathbf{j} \times \mathbf{B} + \nu \nabla^2 \mathbf{u}. \quad (4.1.1)$$

Note that since $\mu \mathbf{j} = \nabla \times \mathbf{B}$,

$$\frac{1}{\rho} \mathbf{j} \times \mathbf{B} = \frac{1}{\mu\rho} (\nabla \times \mathbf{B}) \times \mathbf{B}. \quad (4.1.2)$$

Effects of Lorentz force

The Lorentz force can impede convection when it is strong. This is why sunspots are darker than the solar photosphere. Strong magnetic fields in the sunspot block convective heat transport there making the sunspot relatively dark.

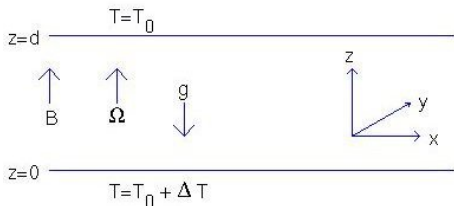
The Lorentz force can act as a restoring force, giving rise to waves, called Alfvén waves.

When combined with the Coriolis force, the Lorentz force gives rise to new waves, MAC waves (MAC: Magnetic, Archimedean and Coriolis forces).

Kinematic dynamos grow exponentially: the Lorentz force stops them growing by changing the flow, causing the dynamo to saturate at a finite field strength.

Rotating magnetconvection: plane layer

The rotating plane layer with a vertical magnetic field



Rotation and magnetic field parallel to gravity, centrifugal acceleration negligible.

A Rayleigh-Bénard convection cell with a liquid metal (Gallium or liquid sodium) is put on a rotating turntable. Strong vertical magnetic field imposed externally.

Chandrasekhar, 1961. The equation of motion is

$$\frac{\partial \mathbf{u}}{\partial t} + 2\Omega \hat{\mathbf{z}} \times \mathbf{u} = -\frac{1}{\rho} \nabla p + g\alpha T' \hat{\mathbf{z}} + \frac{1}{\rho} \mathbf{j} \times \mathbf{B} + \nu \nabla^2 \mathbf{u}. \quad (4.1.3)$$

The temperature equation is

$$\frac{\partial T}{\partial t} + \mathbf{u} \cdot \nabla T = \kappa \nabla^2 T, \quad (4.1.4)$$

and the induction equation is

$$\frac{\partial \mathbf{B}}{\partial t} = \nabla \times (\mathbf{u} \times \mathbf{B}) + \eta \nabla^2 \mathbf{B}, \quad (4.1.5)$$

with

$$\nabla \cdot \mathbf{u} = 0, \quad \nabla \cdot \mathbf{B} = 0 \quad (4.1.6)$$

since the fluid is incompressible.

Since the imposed field is uniform, $\mathbf{B} = B_0 \hat{\mathbf{z}}$, which has no current.

Then $\mathbf{j} \times \mathbf{B} = \mathbf{j} \times B_0 \hat{\mathbf{z}}$, where \mathbf{j} is the current induced by convection, and we assume the magnetic field generated by convection is \mathbf{b} , which is small compared to $B_0 \hat{\mathbf{z}}$.

The induction equation is then

$$\frac{\partial(\mathbf{B}_0 + \mathbf{b})}{\partial t} = \nabla \times (\mathbf{u} \times (\mathbf{B}_0 + \mathbf{b})) + \eta \nabla^2 (\mathbf{B}_0 + \mathbf{b}), \quad (4.1.7)$$

which linearises to

$$\frac{\partial \mathbf{b}}{\partial t} = \nabla \times (\mathbf{u} \times B_0 \hat{\mathbf{z}}) + \eta \nabla^2 \mathbf{b} = B_0 \frac{\partial \mathbf{u}}{\partial z} + \eta \nabla^2 \mathbf{b}. \quad (4.1.8)$$

Non-rotating case 1.

With $\Omega = 0$ the linearised equations are then

$$\frac{\partial \mathbf{u}}{\partial t} = -\frac{1}{\rho} \nabla p + g\alpha T' \hat{\mathbf{z}} + \frac{1}{\rho} \mathbf{j} \times B_0 \hat{\mathbf{z}} + \nu \nabla^2 \mathbf{u}, \quad (4.1.9)$$

$$\frac{\partial T'}{\partial t} = \beta u_z + \kappa \nabla^2 T', \quad (4.1.10)$$

The z component of the induction equation is

$$\frac{\partial b_z}{\partial t} = B_0 \frac{\partial u_z}{\partial z} + \eta \nabla^2 b_z. \quad (4.1.11)$$

The z -component of the double curl of the momentum equation is then

$$\frac{\partial}{\partial t} \nabla^2 u_z = g\alpha \nabla_H^2 T' + \frac{B_0}{\mu\rho} \frac{\partial}{\partial z} \nabla^2 b_z + \nu \nabla^4 u_z. \quad (4.1.12)$$

The simplest case is to look for steady neutral solutions with no time-dependence, so the time-derivative terms are zero.

Non-rotating case 2.

We can then eliminate $\nabla^2 b_z$ from (4.1.12) using (4.1.11), to get

$$0 = g\alpha\nabla_H^2 T' - \frac{B_0^2}{\mu\rho\eta} \frac{\partial^2 u_z}{\partial z^2} + \nu\nabla^4 u_z \quad (4.1.13)$$

and we eliminate T' using the temperature equation (4.1.10). We non-dimensionalise as usual, and two dimensionless parameters emerge.

$$R = \frac{g\alpha\Delta T d^3}{\kappa\nu}, \quad Q = \frac{B_0^2 d^2}{\mu\rho\nu\eta}, \quad (4.1.14)$$

are the usual Rayleigh number and Q is called the Chandrasekhar number, which measures the field strength. With stress-free, constant temperature boundaries, $u_z = \sin \pi z \exp i(k_x x + k_y y)$ is a solution, and if $a^2 = k_x^2 + k_y^2$, we get

$$R_{steady} = \frac{\pi^2 + a^2}{a^2} [(\pi^2 + a^2)^2 + \pi^2 Q], \quad (4.1.15)$$

as the dispersion relation.

Non-rotating magnetoconvection results

This compares with the rotating case result, (2.5.16), with Q in place of E^{-2} . A similar analysis shows that as $Q \rightarrow \infty$, minimum R_{steady} occurs when

$$a \sim \left(\frac{\pi^4}{2}\right)^{1/6} Q^{1/6}, \quad Ra_{steady} \sim \pi^2 Q. \quad (4.1.16)$$

So since a becomes large as magnetic field increases we get tall thin columns.

Since the critical Rayleigh number increases as $Q \rightarrow \infty$, magnetic field suppresses convection. This impeding effect of the magnetic field is why sunspots are dark, the heat transport being reduced.

If $\kappa < \eta$, normally the case in planetary cores, steady modes are the first to onset, but if $\kappa > \eta$ oscillatory modes are possible.

Alfvén waves

In the limit of no diffusion and uniform temperature $T' = 0$, equations (4.1.11) and (4.1.12) are

$$\frac{\partial b_z}{\partial t} = B_0 \frac{\partial u_z}{\partial z}, \quad (4.1.17)$$

and the z-component of the double curl of the momentum equation is then

$$\frac{\partial}{\partial t} \nabla^2 u_z = + \frac{B_0}{\mu \rho} \frac{\partial}{\partial z} \nabla^2 b_z. \quad (4.1.18)$$

Look for wave like solution $\sim \exp i(k_x x + k_y y + k_z z - \omega t)$, and we find wave solutions with

$$\omega^2 = \frac{B_0^2}{\mu \rho} k_z^2 \quad (4.1.19)$$

which are Alfvén waves travelling with the Alfvén speed

$$c = \frac{\omega}{k_z} = \frac{B_0}{\sqrt{\mu \rho}}. \quad (4.1.20)$$

Magnetic field lines as stretched strings

Since the waves travel along the field lines, it is helpful to think of magnetic field lines like stretched strings.

If you give the field an initial perturbation, it responds by sending waves along the field lines, just as a stretched string would.

The Lorentz force can be written

$$\frac{1}{\mu}(\nabla \times \mathbf{B}) \times \mathbf{B} = (\mathbf{B} \cdot \nabla)\mathbf{B}/\mu - \nabla \mathbf{B}^2/2\mu. \quad (4.1.21)$$

The first term is called the curvature force. It is active when field lines are curved.

The second term is called magnetic pressure, and it adds to the gas pressure.

Convection with rotation and magnetic field 1.

We go back to equations (4.1.3) to (4.1.6) and linearise

$$\frac{\partial \mathbf{u}}{\partial t} + 2\Omega \hat{\mathbf{z}} \times \mathbf{u} = -\frac{1}{\rho} \nabla p + g\alpha T' \hat{\mathbf{z}} + \frac{1}{\rho} \mathbf{j} \times B_0 \hat{\mathbf{z}} + \nu \nabla^2 \mathbf{u}, \quad (4.1.22)$$

$$\frac{\partial T'}{\partial t} = \beta u_z + \kappa \nabla^2 T', \quad (4.1.23)$$

$$\frac{\partial \mathbf{b}}{\partial t} = B_0 \frac{\partial \mathbf{u}}{\partial z} + \eta \nabla^2 \mathbf{b}. \quad (4.1.24)$$

Vorticity equation is

$$\frac{\partial \zeta}{\partial t} - 2\Omega \frac{\partial \mathbf{u}}{\partial z} = g\alpha \nabla \times T' \hat{\mathbf{z}} + \frac{B_0}{\rho} \frac{\partial \mathbf{j}}{\partial z} + \nu \nabla^2 \zeta, \quad (4.1.25)$$

$$\frac{\partial \mathbf{j}}{\partial t} = B_0 \frac{\partial \zeta}{\partial z} + \eta \nabla^2 \mathbf{j}. \quad (4.1.26)$$

We might expect rotation and magnetic together to be even more stabilising, but this is not true.

We look for steady solutions as before, with the usual horizontal dependence $\sim \exp i(k_x x + k_y y)$ with $k_x^2 + k_y^2 = a^2$, and non-dimensionalise using d , d^2/η as the unit of length and time.

The dimensionless parameters appearing are now

$$\Lambda = \frac{B_0^2}{\mu\rho\Omega\eta}, \quad E = \frac{\nu}{\Omega d^2}, \quad R^* = \frac{g\alpha\Delta T d}{\kappa\Omega}. \quad (4.1.27)$$

Λ is called the Elsasser number, and $\Lambda \sim 1$ in planetary cores. E is the Ekman number we had before (small in planets).

The modified Rayleigh number $R^* = ERa$. This is still large in planets, but not as large as Ra .

If time-dependence is retained, two other Prandtl numbers appear,

$$Pr = \frac{\nu}{\kappa}, \quad Pm = \frac{\nu}{\eta}. \quad (4.1.28)$$

The hydrodynamic Prandtl number and magnetic Prandtl number respectively.

The magnetic Prandtl number is $Pm \sim 10^{-5}$ in planetary cores, whereas $Pr \approx 0.1$.

If the buoyancy is due to light material rather than temperature, the effective Prandtl number (the Schmidt number ν/κ_{diff}) is large.

Our equations now become

$$E(D^2 - a^2)\zeta + 2Du_z + \Lambda Dj_z = 0, \quad (4.1.29)$$

$$E(D^2 - a^2)^2 u_z - 2D\zeta + \Lambda(D^2 - a^2)Db_z - R^* a^2 T' = 0, \quad (4.1.30)$$

$$(D^2 - a^2)b_z + Du_z = 0, \quad (4.1.31)$$

$$(D^2 - a^2)j_z + D\zeta = 0, \quad (4.1.32)$$

$$(D^2 - a^2)T' + u_z = 0, \quad (4.1.33)$$

where $\zeta = \boldsymbol{\zeta} \cdot \hat{\mathbf{z}}$, $D = d/dz$ and a is the horizontal wavenumber.

The case with stress-free, electrically insulating and constant temperature boundaries,

$$D^2 u_z = u_z = D\zeta = j_z = T' = 0 \quad \text{on} \quad z = 0, 1, \quad (4.1.34)$$

gives $u_z = \sin \pi z$ solutions.

The expression for the modified Rayleigh number is now

$$R^* = \frac{\pi^2 + a^2}{a^2} \left[\frac{[E(\pi^2 + a^2)^2 + \Lambda\pi^2]^2 + 4\pi^2(\pi^2 + a^2)}{E(\pi^2 + a^2)^2 + \Lambda\pi^2} \right]. \quad (4.1.35)$$

If Λ is very small, this reduces to the purely rotating case, for which at small E we have $a \sim E^{-1/3}$ and $R^* \sim E^{-1/3}$, which is large.

But if Λ is $O(1)$, then the E terms are negligible, and then a and R^* are also $O(1)$, which is smaller than $O(E^{-1/3})$. So the effect of the magnetic field is to reduce the critical Rayleigh number, i.e. it helps convection.

The magnetic field is breaking the Taylor-Proudman constraint, and so allowing convection to occur on larger horizontal length-scales. This could be important in planetary dynamos.

Field and rotation axes at different angles

The classic problem has the rotation vector and the magnetic field aligned with gravity. There have been studies where the rotation vector and the magnetic field are no longer aligned.

In the case where they are mutually perpendicular, appropriate near the equator of a planet, rolls can line up either with the rotation, the field or neither, depending on the parameters.

These problems are complicated because of the many parameters and angles involved, but they all reduce to systems of ODEs, which are straightforward to solve numerically.

The problem has also been considered in spherical geometry. This is more challenging numerically, but the overall picture is similar.

It is normally the case that there is a critical Elsasser number Λ_c .

For $\Lambda < \Lambda_c$ rotation is dominant, and we get tall thin columns and a high critical Rayleigh number.

For $\Lambda > \Lambda_c$ magnetic field breaks the Taylor-Proudman constraint, and wider columns occur, with a lower critical Rayleigh number.

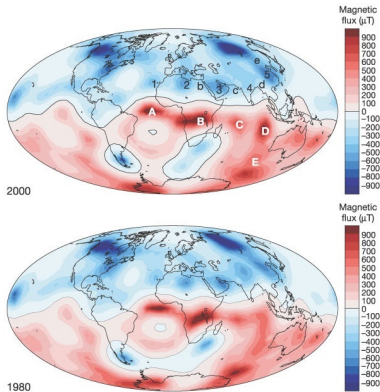
For more complicated magnetic fields, magnetically driven instabilities can occur.

4.2 Waves in rotating MHD

Geomagnetic field and Secular Variation

Geomagnetic field is described in terms of the Gauss coefficients of the spherical harmonic expansion outside the core $\mathbf{B} = -\nabla\Psi$.

$$\Psi = r_s \sum_{n=1}^{\infty} \sum_{m=0}^{m=n} \left(\frac{r_s}{r}\right)^{n+1} P_n^m(\cos\theta)(g_n^m \cos m\phi + h_n^m \sin m\phi).$$



Magnetic field B_r measured at the surface, but mantle insulating, so can extrapolate field B_r to Core-Mantle boundary (CMB).

Radial geomagnetic field at CMB in 1980 and 2000. Wave-like behaviour seen.

Small changes occur in 20 years. Secular variation is first time-derivative of geomagnetic field. Some Westward drift is visible.

Types of waves in the core

P-waves

Inertial waves

Torsional waves

Magnetic Rossby waves

S-waves

Internal gravity waves

MAC waves

Dynamo waves

So many different waves! How do we make sense of them?

S-waves and P-waves are seismic waves, excited by earthquakes and detected by seismometers. Travel very fast, 3-8 km/sec.

All except S-waves occur in a fluid. P-waves depend on compressibility. All the other fluid waves occur in incompressible fluid, $\nabla \cdot \mathbf{u} = 0$.

Inertial waves occur in rotating fluids, internal gravity waves in density stratified fluids.

MAC waves, Torsional waves and magnetic Rossby waves are all rotating MHD waves. Dynamo waves are the kinematic waves in dynamo theory.

We consider a small piece of core, rotating with angular velocity $\Omega \hat{\mathbf{z}}$, with uniform magnetic field \mathbf{B}_0 (any direction).

We then give the fluid a small velocity perturbation of the form $\mathbf{u} = \mathbf{u}_0 \exp i(\mathbf{k} \cdot \mathbf{x} - \omega t)$ wavevector \mathbf{k} , frequency ω .

Wave travels in \mathbf{k} -direction. $\nabla \cdot \mathbf{u} = 0$ so $\mathbf{u}_0 \cdot \mathbf{k} = 0$, transverse waves.

We insert the wave form into the equation of motion and the induction equation, then work out the dispersion relation between ω and \mathbf{k} .

Equation of motion

Linearised equation of motion for adiabatic inviscid fluid

$$\frac{\partial \mathbf{u}}{\partial t} + 2\boldsymbol{\Omega} \times \mathbf{u} = -\nabla p' / \rho + \frac{1}{\rho} \mathbf{j} \times \mathbf{B}_0 \quad (4.2.1)$$

Inertia Coriolis accn Pressure Lorentz force

If fluid is stably stratified (not adiabatic) there is an extra buoyancy term.

Magnetic field equation (induction equation)

$$\frac{\partial \mathbf{b}}{\partial t} = (\mathbf{B}_0 \cdot \nabla) \mathbf{u} + \eta \nabla^2 \mathbf{b}, \quad \mu \mathbf{j} = \nabla \times \mathbf{b}, \quad (4.2.2)$$

Ignore magnetic diffusion in simple theory (magnetic Reynolds number 1000).

Dispersion relation for rotating MHD waves 1.

Eliminate pressure by taking curl of equation of motion, to get the vorticity ζ equation.

$$\frac{\partial \zeta}{\partial t} - 2(\boldsymbol{\Omega} \cdot \nabla) \mathbf{u} = \frac{1}{\rho} (\mathbf{B}_0 \cdot \nabla) \mathbf{j}, \quad \zeta = \nabla \times \mathbf{u}. \quad (4.2.3)$$

Take time-derivative and eliminate \mathbf{j} using the curl of the induction equation

$$\frac{\partial^2 \zeta}{\partial t^2} - 2(\boldsymbol{\Omega} \cdot \nabla) \frac{\partial \mathbf{u}}{\partial t} = \frac{1}{\mu \rho} (\mathbf{B}_0 \cdot \nabla)^2 \zeta, \quad (4.2.4)$$

Now insert $\mathbf{u} = \mathbf{u}_0 \exp i(\mathbf{k} \cdot \mathbf{x} - \omega t)$ to get

$$\left(\frac{(\mathbf{B}_0 \cdot \mathbf{k})^2}{\mu \rho} - \omega^2 \right) \zeta = 2(\boldsymbol{\Omega} \cdot \nabla) \frac{\partial \mathbf{u}}{\partial t} \quad (4.2.5)$$

Now take the curl of this, using $\nabla \times \zeta = -\nabla^2 \mathbf{u}$, to get

$$- \left(\frac{(\mathbf{B}_0 \cdot \mathbf{k})^2}{\mu \rho} - \omega^2 \right) \nabla^2 \mathbf{u} = 2(\boldsymbol{\Omega} \cdot \nabla) \frac{\partial \zeta}{\partial t} \quad (4.2.6)$$

and now use (4.2.5) to get

Dispersion relation for rotating MHD waves 2.

the dispersion relation

$$4\omega^2(\boldsymbol{\Omega} \cdot \mathbf{k})^2 = \left(\frac{(\mathbf{B}_0 \cdot \mathbf{k})^2}{\mu\rho} - \omega^2 \right)^2 \mathbf{k}^2,$$

with solution $\omega = \frac{(\boldsymbol{\Omega} \cdot \mathbf{k}) \pm \sqrt{(\boldsymbol{\Omega} \cdot \mathbf{k})^2 + \mathbf{k}^2(\mathbf{B}_0 \cdot \mathbf{k})^2/\mu\rho}}{|\mathbf{k}|}$. (4.2.7)

There are a lot of waves in this formula!

Start by setting $\mathbf{B}_0 = 0$. Then

$$\omega = \frac{2(\boldsymbol{\Omega} \cdot \mathbf{k})}{|\mathbf{k}|} = \omega_c. \quad (4.2.8)$$

These are Poincaré waves or inertial waves. Period generally a bit longer than $2\pi/2\Omega = 12$ hours.

Now restore \mathbf{B}_0 . Plus sign gives fast magneto-inertial waves. These waves travel faster than the inertial waves, because the magnetic field adds to the restoring force.

Minus sign is more interesting, define

$$\omega_M = \frac{(\mathbf{B}_0 \cdot \mathbf{k})}{(\mu\rho)^{1/2}}. \quad (4.2.9)$$

$2\pi/\omega_m \sim 6$ years in the core. This is the Alfvén time, the time it takes for an Alfvén to go back and forth in the core.

Generally in planets $\omega_C \gg \omega_M$.

We can now write

$$\omega = \frac{(\boldsymbol{\Omega} \cdot \mathbf{k}) \pm \sqrt{(\boldsymbol{\Omega} \cdot \mathbf{k})^2 + \mathbf{k}^2(\mathbf{B}_0 \cdot \mathbf{k})^2/\mu\rho}}{|\mathbf{k}|}.$$

as

$$\omega = \frac{\omega_c}{2} \pm \frac{\omega_c}{2} \sqrt{1 + \frac{4\omega_m^2}{\omega_c^2}}. \quad (4.2.10)$$

Then binomial expansion gives

$$\omega = \omega_{MC} = \frac{\omega_M^2}{\omega_C} + \dots \quad (4.2.11)$$

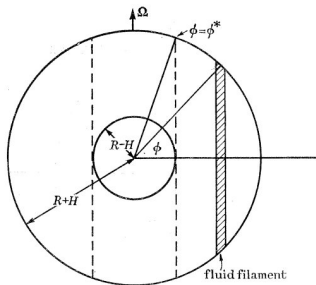
which in general corresponds to a period of thousands of years. These are the slow MC waves. If the buoyancy term is included they become MAC waves (M magnetic, A Archimedean, C Coriolis). Too slow to see directly in the SV signal, but may be important on dynamo time-scales.

Slow magnetic Rossby waves

Recall that quasi-geostrophic motions with k_z small can have periods of months rather than days, i.e. smaller ω_C .

So for these waves $\omega_{MC} = \omega_M^2 / \omega_C$ is larger than usual, so periods may be hundreds of years or maybe even just decades.

These are the slow magnetic Rossby waves, a special QG class of the slow MC waves.



Hide showed that in spherical geometry these slow magnetic Rossby waves have a quasi-geostrophic columnar structure.

Recently shown (Hori et al. 2015, 2017) that these occur in dynamo simulations and may be seen in the SV signal.

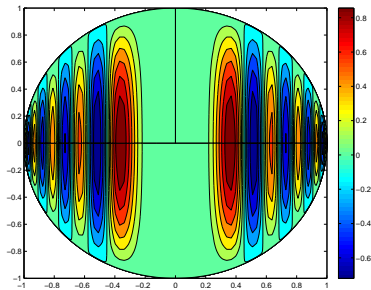
Magnetic Rossby Waves

Magnetic Rossby waves in a sphere can be solved exactly for the special Malkus field $\mathbf{B}_0 = B_0 s \hat{\phi}$. Cylindrical coordinates (s, ϕ, z) .

Not very Earth-like field, but gives idea of what they look like.

The solution is too complex to go through here: details in Malkus 1967, J Fluid Mech. 28, p793.

Magnetic Rossby Waves



Meridional plane section of u_r with $m = 8$ ($\exp im\phi$). Malkus field $\mathbf{B}_0 = B_0 s \hat{\phi}$. Cylindrical coordinates (s, ϕ, z) .

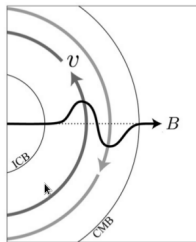
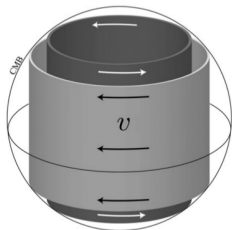
For each m there are modes with N_s rolls in the s -direction and N_z rolls in the z -direction. Magnetic Rossby waves have $N_z = 1$.

Modes which have N_s large and m moderate have only a small amount of vortex stretching, so have frequencies faster than the ten thousand year period of 'normal' MC waves.

4.3 Torsional waves in the core

Rotating MHD waves: Torsional Oscillations

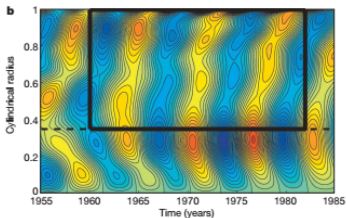
There is a special class of waves with $\boldsymbol{\Omega} \cdot \mathbf{k} = 0$. They are geostrophic waves, with the Coriolis force balanced entirely by pressure gradient. These modes don't stretch the vortex lines. The restoring force is just Lorentz force, so these are torsional oscillations (TOs). In the Earth's core, they have a period of about 6 years.



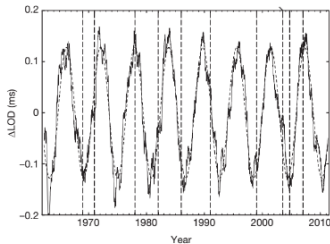
Torsional waves transport angular momentum. This gets transferred to the mantle, resulting in small but observable length of day changes.

Torsional oscillation observations

(a) Gillet et al 2010:



(b) Holme & de Viron 2013



(a) The axisymmetric part of u_ϕ constructed from observations of the geomagnetic field.

(b) Length-of-day variations. Since total angular momentum is conserved, torsional waves change the mantle rotation rate.

An approximately six year period is seen in both data sets. Waves propagate out from the tangent cylinder, the cylinder surrounding the Earth's solid inner core.

Dynamo model equations

$$\frac{\partial \mathbf{u}}{\partial t} + (\mathbf{u} \cdot \nabla) \mathbf{u} = -\frac{Pm}{E} [\nabla p + 2\hat{\mathbf{z}} \times \mathbf{u} - (\nabla \times \mathbf{B}) \times \mathbf{B}] + \frac{Pm^2 Ra}{Pr} T \mathbf{r} + Pm \nabla^2 \mathbf{u} \quad (4.3.1)$$

$$\frac{\partial T}{\partial t} + (\mathbf{u} \cdot \nabla) T = \frac{Pm}{Pr} \nabla^2 T + \epsilon, \quad \frac{\partial \mathbf{B}}{\partial t} - \nabla \times (\mathbf{u} \times \mathbf{B}) = \nabla^2 \mathbf{B} \quad (4.3.2, 3)$$

$$\nabla \cdot \mathbf{u} = 0, \quad \nabla \cdot \mathbf{B} = 0 \quad (4.3.4)$$

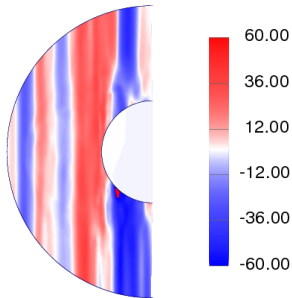
$$E = \frac{\nu}{\Omega D^2}, \quad Ra = \frac{g\alpha|\epsilon|D^5}{\nu\kappa\eta}, \quad Pr = \frac{\nu}{\kappa}, \quad Pm = \frac{\nu}{\eta}. \quad (4.3.5)$$

Boundary conditions used: no-slip, fixed flux; insulating magnetic.

Zero compositional flux at CMB, uniform sink in interior.

Parameters used: $E \in [10^{-6}, 10^{-4}]$, $Ra/Ra_c = 8.3$, $Pr = 1$, $Pm \in [1, 5]$, radius ratio = 0.35 These give 'Earth-like' dynamo models: basically dipolar but with an appropriate amount of reversed flux patches.

Torsional Oscillations movie



Time-lapse movie of the axisymmetric part of u_ϕ on a meridional section. $E = 10^{-5}$.

The solid inner core of the Earth doesn't take part in the oscillations in these simulations.

Alfvén wave equation in spherical geometry is

$$\frac{\partial^2}{\partial t^2} \left(\frac{u_\phi}{s} \right) = \frac{1}{s^3 h} \frac{\partial}{\partial s} \left(s^3 h U_A^2 \frac{\partial}{\partial s} \left(\frac{u_\phi}{s} \right) \right) \quad (4.3.6)$$

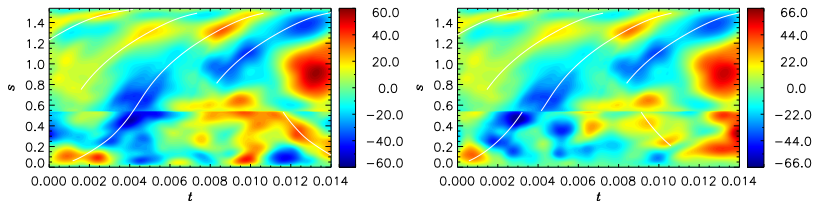
where $U_A^2 = \overline{\langle B_s^2 / \mu \rho \rangle}$, the bar denoting ϕ average and angle brackets z -average. $h(s)$ is height of cylinder.

We run the dynamo simulation, and when initial transients have gone, we run for a further time τ , and evaluate U_A from B_s , the field averaged over time τ .

We make plots in the t - s plane of the fluctuating part of u_ϕ , i.e. $u'_\phi = u_\phi - \widetilde{u}_\phi$ where \widetilde{u}_ϕ is the time-average over the whole τ run.

We then look for features in u'_ϕ propagating with the Alfvén speed.

Torsional Oscillations detected



Left: Inside Tangent Cylinder North. Right: Inside Tangent Cylinder South. $\langle \overline{u_\phi} \rangle'$, $E = 10^{-4}$, $Pm = 5$. White curves have gradient U_A . Similar pictures for $E = 10^{-5}$.

Plus points: torsional oscillations found in dynamo simulations. Mostly (but not exclusively) travel outwards. When field is scaled to observed B_r at the CMB, travel time from tangent cylinder to equator is about 3 years, similar to Gillet et al. data.

Minus points: Origin inside the tangent cylinder rather than at the TC. Waves not as periodic as suggested by the Gillet et al. data.

Magnetoconvection simulations

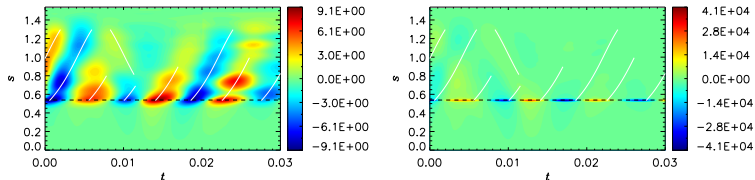
In geodynamo simulations the importance of the Reynolds stress is overestimated: kinetic and magnetic energy is typically similar, whereas magnetic energy is much larger than kinetic energy in the core.

Also, the need to generate a magnetic field places severe restrictions on the accessible parameter space, e.g. very expensive to lower Pm .

So we used **Magnetoconvection** simulations. Same code, but change magnetic boundary condition: impose a dipole magnetic field at the core-mantle boundary and/or inner-core boundary.

Saves CPU time: don't have to wait for field to build up. Allows lower E , much lower Pm and can get into dominant magnetic energy regime.

Magnetoconvection results



$E = 5 \times 10^{-6}$, $Pm = 0.1$, $Ra = 5Ra_c$, $\Lambda \approx 100$.

Left: u'_ϕ contours. Right: F'_L contours. F'_R negligible.

In this strong field, low E case, TO's are much more periodic, and originate from the tangent cylinder and propagate outwards. No significant reflection.

Summary on Torsional Oscillations

TOs observed in the core from secular variation and LOD signal.

Can be modelled using dynamo and magnetoconvection codes.

They originate from quite small scale (~ 400 km) convection, which has turnover time and period ~ 6 years.

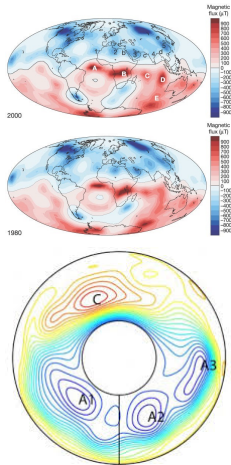
The convection is broad-band in azimuthal wavenumber and has an $m = 0$ component.

The convection disturbs the TC shear layer, and this forces the TOs which propagate outwards.

4.4 Magnetic Rossby waves in the core?

Secular Variation: waves or flow?

We now consider the nonaxisymmetric modes and their connection with the secular variation.



Atlantic hemisphere

- Are these patches of magnetic field advected by an approximately steady flow, or are they magnetic Rossby waves?
- Most, but not all of the signal can be fitted with a steady flow, the eccentric gyre, shown in equatorial plane
- This flow is believed to be fairly z-independent. Carries the equatorial flux patches westward in the Atlantic hemisphere, while flow is eastward under the Pacific. Recent evidence of fast flow at high latitudes under Siberia.
- There are definite features which cannot be explained by a steady flow.

Magnetic Rossby waves in a thick shell

The axial z-component of the vorticity equation is

$$\rho \frac{d\zeta}{dt} - 2\rho\Omega \frac{\partial u'_z}{\partial z} = \hat{e}_z \cdot \nabla \times (j' \times \tilde{B}) \quad (4.4.1)$$

where $\zeta' = \nabla \times u'$ is the vorticity and \tilde{B} is the mean field. In the simulations the azimuthal wavelength is shorter than the radial or axial wavelengths, or the mean length scales. We integrate over z , and use $\zeta \approx -(1/s)(\partial u'_s/\partial\phi)$ to get

$$\frac{d}{dt} \left[\frac{d}{dt} \frac{1}{2H} \int_{-H}^{+H} \frac{1}{s} \frac{\partial u'_s}{\partial\phi} dz - \frac{2\Omega s}{r_o^2 - s^2} u'_s \right] = \frac{1}{2\rho\mu_0 H} \int_{-H}^{+H} \frac{\overline{B_\phi^2}}{s^3} \frac{\partial^3 u'_s}{\partial\phi^3} dz \quad (4.4.2)$$

Magnetic Rossby waves in a thick shell

Look for waves $\exp\{i(m\phi - \omega t)\}$.

Magnetic Rossby waves have negligible inertial term, so the most right-hand term can be neglected.

We need to remember that

$$\frac{d}{dt} = \frac{\partial}{\partial t} + \frac{\hat{U}_\phi}{s} \frac{\partial}{\partial \phi}$$

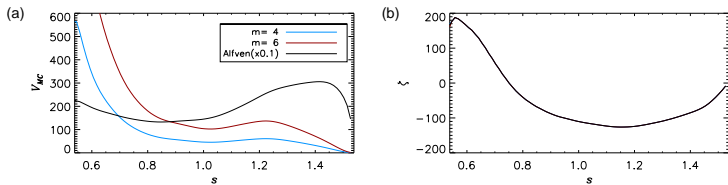
so

$$\frac{\omega}{m} = \frac{\hat{U}_\phi}{s} - \frac{m^2(r_0^2 - s^2)\hat{B}_\phi^2}{2\Omega\mu\rho s^4}. \quad (4.4.3)$$

Magnetic Rossby waves go westward relative to mean flow advection speed \hat{U}_ϕ .

Advection speed similar to the wave speed in the Earth's core.

Magnetic Rossby wave frequencies

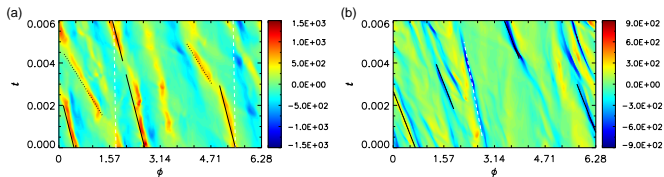


The left plot is the wave speed and the right figure is the azimuthal flow speed from a dynamo simulation with $E = 10^{-5}$, $Pm = 5$, $Ra = 8.32Ra_c$. V_{MC} is phase speed of magnetic Rossby waves, $\zeta = \hat{U}_\phi/s$ is advection angular velocity.

$$V_{MC} = \frac{m^2(r_0^2 - s^2)B_\phi^2}{2\Omega\mu\rho s^4}.$$

Both similar, but flow dominates near equator, waves dominate at higher latitudes. Higher latitudes where to seek waves? Large m better, but $m > 13$ can't be detected.

Rossby waves in simulations



$$E = 10^{-5}, Pm = 5, Ra = 8.32Ra_c$$

Technique same as for TOs: remove time average part and plot the z -averaged part of u_s .

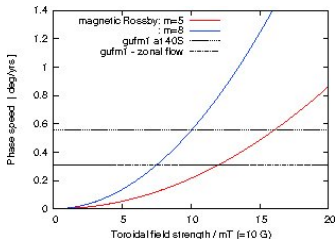
Left: $\phi - t$ plot of $\langle u_s \rangle$ at $s = 0.5r_o$ (latitude 60°). Right: same at $s = 0.766r_o$.

White dashed: advection speed.

Left: Black solid is wave speed + advection speed for $m = 5$ and Black dashed is $m = 8$. Right solid is $m = 6$.

At higher latitudes, waves + flow correlate well. At low latitudes, hard to distinguish.

Comparing with data



At 40° S, upper black line is drift speed from observational model gufm1, lower black line is drift speed with core flow removed (Hulot et al. 2002). Difference $\approx 0.2^\circ$ per year.

The coloured dashed lines are the expected wave speeds from our model as a function of the z-averaged toroidal field.

Indicates that the azimuthal field is a lot stronger than the poloidal field of 3 mT if there is a wave component to the secular variation

Conclusions on Magnetic Rossby waves

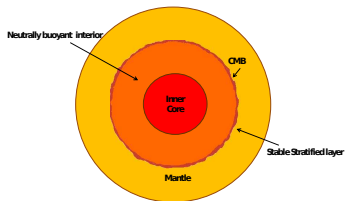
- Magnetic Rossby waves can be seen in dynamo simulations
- Waves are generally slow, so the wave drift will be dominated by advection at lower latitudes.
- Best chance of separating the waves from the advection velocity is at high latitudes, where the wave speed is significant compared to the flow speed.

Difficulty is that waves are quite nonlinear.

- Need to analyse the data to see the wave speeds of the different wavenumbers: dispersion relation depends on ratio of wave/advection speed.

4.5 Shallow water MHD model

Stable layer in the Earth's core?



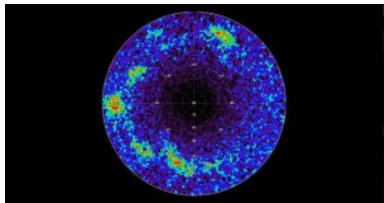
Earth's core with stable layer

Helffrich & Kaneshima (2010) found a layer at the top of the liquid outer core where seismic waves are slower than in rest of outer core. Interpreted as a stable layer few hundred km thick.

Braginsky (1984, 1993) suggested light material released as the solid inner core grows would accumulate under the core mantle boundary: inverted ocean of the core. Even if the core is compositionally mixed, there could be a thermally stably stratified layer below the CMB.

Axisymmetric core oscillations visible in both secular variation and length of day observations. 6 year period due to torsional Alfvén oscillations in whole core, but Buffett (2015) suggested the 60 year period could be MAC waves in the stably stratified layer.

Waves in the tachocline?



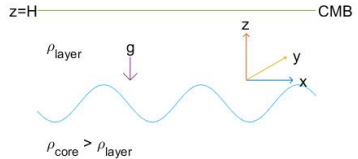
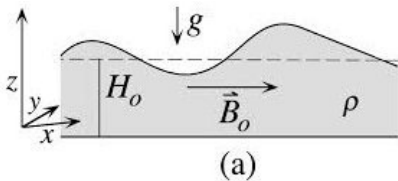
*Bright points in the Solar Corona,
viewed from N. Pole using Stereo*

McIntosh et al. 2017. Bright points in the corona show a large scale slow wave-like motion, with very slow wavespeed, ~ 3 m/sec.

Slower than any waves in the corona. Suggestion is that there are magnetic Rossby waves in the stably stratified tachocline. These are coupled through the magnetic field to the bright points in the corona.

These waves may be linked to dynamo action in the Sun.

Shallow water MHD model



Perfectly conducting fluid, so the wavy boundary is a field line.

When applied to a stably stratified layer in the core, picture is upside down, with wavy boundary being the interface between the low density layer fluid and higher density outer core fluid. Rigid boundary at the CMB is then above the wavy boundary.

Magnetic field configuration

We concentrate on simplest problem, an azimuthal field symmetric about the equator $\mathbf{B} = B_0 \sin \theta \hat{\phi}$. Now have fairly complete picture of this case.

Applications have radial fields as well, but these can transmit energy in and out of the layer through Alfvén waves.

Also found significant differences if the azimuthal field has an internal zero, e.g. $\mathbf{B} = B_0 \sin \theta \cos \theta \hat{\phi}$.

Antisymmetric components of azimuthal field are expected in the Earth and the Sun.

Spherical shell of radius R_0 , coordinates (r, θ, ϕ) , rotating with angular speed Ω_0 , with gravity $-g\hat{\mathbf{r}}$ and azimuthal magnetic field $\mathbf{B} = B_0(\theta)\hat{\phi}$.

The shell has a thin layer of electrically conducting fluid of depth H , $H \ll R_0$.

We look at waves and instabilities in this system, using shallow water MHD. Longuet-Higgins (1968) gave a full description of the waves in the $B_0 = 0$ case.

Mathematically equivalent to a thin stably stratified layer of fluid: $gH/R_0^2 \rightarrow N^2$, where N is the buoyancy frequency.

$$\frac{\partial \mathbf{B}}{\partial t} + (\mathbf{u} \cdot \nabla) \mathbf{B} = (\mathbf{B} \cdot \nabla) \mathbf{u} \quad (4.5.1)$$

$$\frac{\partial \mathbf{u}}{\partial t} + (\mathbf{u} \cdot \nabla) \mathbf{u} + 2\boldsymbol{\Omega} \times \mathbf{u} = \frac{1}{\mu_0 \rho} (\mathbf{B} \cdot \nabla) \mathbf{B} - g \nabla H \quad (4.5.2)$$

$$\frac{\partial H}{\partial t} + \nabla \cdot (H \mathbf{u}) = 0 \quad (4.5.3)$$

$$\nabla \cdot (H \mathbf{B}) = 0 \quad (4.5.4)$$

In these equations \mathbf{u} and \mathbf{B} represent the horizontal components of the velocity and magnetic field respectively. The operator ∇ is the horizontal gradient, ρ is the density of the fluid, μ_0 is the permeability of free space and H is the thickness of the layer.

In (4), its **horizontal** divergence, so no contradiction with \mathbf{B} being divergence free in 3D.

Linearised equations

Waves $\sim \exp i(m\phi - \omega t)$. Scale frequency with $2\Omega_0$, so

$$\lambda = \omega/2\Omega_0.$$

$H = H_0 + h$, h scaled as $\eta = gh/4\Omega^2 R_0^2$, change of variable:

$\mu = \cos \theta$. Differential operator $D = -\sin \theta \partial / \partial \theta = (1 - \mu^2) \partial / \partial \mu$.

$$-\lambda u_\theta + \mu u_\phi + D\eta - m\alpha^2 b_\theta - 2\alpha^2 \mu b_\phi = 0 \quad (4.5.5)$$

$$\lambda u_\phi - \mu u_\theta - m\eta + m\alpha^2 b_\phi + 2\alpha^2 \mu b_\theta = 0 \quad (4.5.6)$$

$$\lambda \epsilon (1 - \mu^2) \eta + Du_\theta - mu_\phi = 0 \quad (4.5.7)$$

$$\lambda b_\theta + mu_\theta = 0 \quad (4.5.8)$$

$$\lambda b_\phi + mu_\phi = 0. \quad (4.5.9)$$

Two key parameters

$$\epsilon = \frac{4\Omega_0^2 R_0^2}{gH_0}, \quad \alpha^2 = \frac{v_A^2}{4\Omega_0^2 R_0^2}, \quad \text{where } v_A^2 = \frac{B_0^2}{\mu_0 \rho}, \quad \lambda = \frac{\omega}{2\Omega_0}. \quad (4.5.10)$$

Determining the Eigenvalues and Eigenvectors

The solutions for the dependent variables are expansions of Associated Legendre Polynomials,

$$u_\theta = \sum_{n=m}^{\infty} A_n^m P_n^m(\mu), \quad b_\theta = \sum_{n=m}^{\infty} B_n^m P_n^m(\mu), \quad u_\phi = \sum_{n=m}^{\infty} C_n^m P_n^m(\mu),$$

$$b_\phi = \sum_{n=m}^{\infty} D_n^m P_n^m(\mu), \quad \eta = \sum_{n=m}^{\infty} E_n^m P_n^m(\mu). \quad (4.5.11)$$

Insert truncated expansions into equations \rightarrow matrix eigenvalue problem for λ . Wave types found:

Magneto-Inertial Gravity waves : Magneto-Kelvin waves
(MIG waves)

Fast magnetic Rossby waves: Slow magnetic Rossby waves

The equation for u_θ can be written

$$\begin{aligned}
 & (1 - \mu^2) \frac{\partial^2 u_\theta}{\partial \mu^2} + \frac{2m^2}{(\lambda^2 - \alpha^2 m^2)\epsilon(1 - \mu^2) - m^2 \mu} \frac{\partial u_\theta}{\partial \mu} \\
 & + \left\{ \epsilon(\lambda^2 - \alpha^2 m^2) - \frac{m(\lambda + 2m\alpha^2)}{(\lambda^2 - \alpha^2 m^2)} - \epsilon \frac{(\lambda + 2m\alpha^2)^2}{(\lambda^2 - \alpha^2 m^2)} \mu^2 \right. \\
 & \left. - \frac{m^2}{1 - \mu^2} - \frac{2\epsilon m(\lambda + 2m\alpha^2)\mu^2}{(\lambda^2 - \alpha^2 m^2)\epsilon(1 - \mu^2) - m^2} \right\} u_\theta = 0, \quad (4.5.12)
 \end{aligned}$$

and the equation for η is

$$\begin{aligned}
 & (1 - \mu^2) \frac{\partial^2 \eta}{\partial \mu^2} + 2 \left(\frac{(\lambda + 2m\alpha^2)^2 (1 - \mu^2)}{(\lambda^2 - m^2 \alpha^2)^2 - (\lambda + 2m\alpha^2)^2 \mu^2} - 1 \right) \mu \frac{\partial \eta}{\partial \mu} \\
 & + \left\{ \frac{-m(\lambda + 2m\alpha^2)}{(\lambda^2 - m^2 \alpha^2)} - \frac{m^2}{1 - \mu^2} + \epsilon \left[(\lambda^2 - m^2 \alpha^2) - \frac{(\lambda + 2m\alpha^2)^2 \mu^2}{\lambda^2 - m^2 \alpha^2} \right] \right. \\
 & \left. + \frac{2m(\lambda + 2m\alpha^2)(\lambda^2 - m^2 \alpha^2)}{(\lambda^2 - m^2 \alpha^2)^2 - (\lambda + 2m\alpha^2)^2 \mu^2} \right\} \eta = 0. \quad (4.5.13)
 \end{aligned}$$

Asymptotic simplification

These equations look complicated, but for ϵ and α small, there are solutions with $\lambda \sim O(\epsilon^{-1/2})$ which is large, then the equation for η

$$\begin{aligned} & (1 - \mu^2) \frac{\partial^2 \eta}{\partial \mu^2} + 2 \left(\frac{(\lambda + 2m\alpha^2)^2 (1 - \mu^2)}{(\lambda^2 - m^2\alpha^2)^2 - (\lambda + 2m\alpha^2)^2 \mu^2} - 1 \right) \mu \frac{\partial \eta}{\partial \mu} \\ & + \left\{ \frac{-m(\lambda + 2m\alpha^2)}{(\lambda^2 - m^2\alpha^2)} - \frac{m^2}{1 - \mu^2} + \epsilon \left[(\lambda^2 - m^2\alpha^2) - \frac{(\lambda + 2m\alpha^2)^2 \mu^2}{\lambda^2 - m^2\alpha^2} \right] \right. \\ & \left. + \frac{2m(\lambda + 2m\alpha^2)(\lambda^2 - m^2\alpha^2)}{(\lambda^2 - m^2\alpha^2)^2 - (\lambda + 2m\alpha^2)^2 \mu^2} \right\} \eta = 0. \end{aligned} \quad (4.5.14)$$

simplifies down to

$$(1 - \mu^2) \frac{\partial^2 \eta}{\partial \mu^2} - 2\mu \frac{\partial \eta}{\partial \mu} + \left\{ \epsilon \lambda^2 - \frac{m^2}{1 - \mu^2} \right\} \eta = 0. \quad (4.5.15)$$

which is the standard associated Legendre equation with well-known solutions.

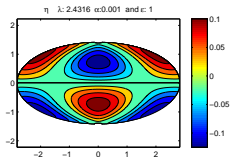
Magneto-Inertial Gravity waves

When ϵ , α are small, we have gravity waves, $\eta \sim P_n^m(\mu)$,

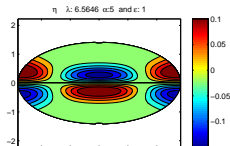
$$\omega = \pm \frac{\sqrt{n(n+1)gH_0}}{R_0} = \pm N\sqrt{n(n+1)}. \quad (4.5.16)$$

If ϵ (rotation) increases, waves slow down and become equatorially trapped. If α (magnetic field) increases, waves speed up, also become equatorially trapped. Eastward and westward branches found.

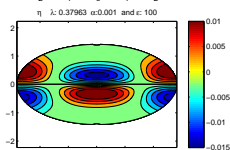
$\alpha = 0.001$
 $\epsilon = 1$



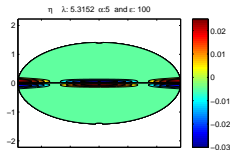
$\alpha = 5$
 $\epsilon = 1$



$\alpha = 0.001$
 $\epsilon = 100$



$\alpha = 5$
 $\epsilon = 100$



At large ϵ with $\alpha \sim O(1)$, there are solutions with $\lambda \sim O(\epsilon^{-1/4})$ which is small.

We now consider the magnitude of the terms in the u_θ equation, and many terms are eliminated, leaving the Parabolic Cylinder function equation, which is a form of Hermite's equation.

$$\frac{d^2 u_\theta}{d\mu^2} + \left\{ (\lambda^2 - \alpha^2 m^2)\epsilon - \frac{m(\lambda + 2m\alpha^2)}{(\lambda^2 - \alpha^2 m^2)} \right\} u_\theta - \frac{\epsilon(\lambda + 2m\alpha^2)^2}{(\lambda^2 - \alpha^2 m^2)} \mu^2 \tilde{u}_\theta = 0, \quad (4.5.17)$$

Rescale

$$\mu = \frac{1}{\sqrt{2}} \left[\frac{(\lambda^2 - \alpha^2 m^2)}{\epsilon(\lambda + 2\alpha^2 m)^2} \right]^{1/4} \hat{\mu}, \quad (4.5.18)$$

The solutions of this equation are the Parabolic Cylinder Functions.

Dispersion Relation

$$\frac{1}{2} \left[\frac{(\lambda^2 - \alpha^2 m^2)}{\epsilon(\lambda + 2\alpha^2 m)^2} \right]^{1/2} \left\{ (\lambda^2 - \alpha^2 m^2)\epsilon - \frac{m(\lambda + 2m\alpha^2)}{(\lambda^2 - \alpha^2 m^2)} \right\} = \nu + \frac{1}{2}, \quad (4.5.19)$$

for $\nu = 0, 1, 2, \dots$

For large ϵ , with $\alpha \sim O(1)$, $\lambda \sim \pm \frac{(2\nu+1)^{1/2}}{\epsilon^{1/4}}$,

Fast Magnetic Rossby waves

At small ϵ we have Rossby waves as well as MIG waves. These have frequency $O(\Omega_0)$, and spherical harmonic solutions. The term $\partial\eta/\partial t$ drops out of the mass conservation equation.

They travel westwards, and at small α

$$\omega = -\frac{2\Omega_0 m}{n(n+1)}.$$

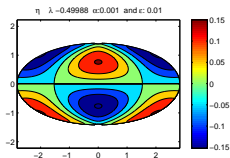
At large ϵ they turn into equatorially trapped waves, described by parabolic cylinder functions.

As α increases, at $\alpha = 0.5$, $\lambda = -0.5m$. For $\alpha > 0.5$, they become super-Alfvénic.

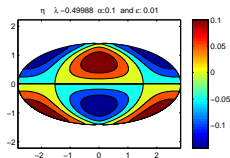
At large α they become polar trapped, described by Whittaker's equation, with associated Laguerre function solutions.

Fast Magnetic Rossby wave eigenfunctions

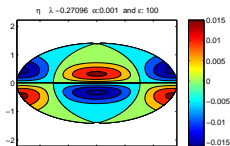
$\alpha = 0.001$
 $\epsilon = 0.01$
 $m = 1$



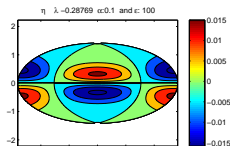
$\alpha = 0.1$
 $\epsilon = 0.01$
 $m = 1$



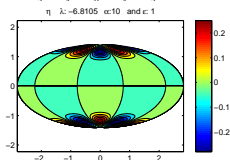
$\alpha = 0.001$
 $\epsilon = 100$
 $m = 1$



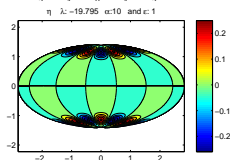
$\alpha = 0.1$
 $\epsilon = 100$
 $m = 1$



$\alpha = 10$
 $\epsilon = 1$
 $m = 2$



$\alpha = 10$
 $\epsilon = 1$
 $m = 3$



Slow Magnetic Rossby waves

These slow waves are in hydromagnetic equilibrium, so inertial term in the equation of motion is negligible. Time-dependence only in induction equation.

Frequency goes to zero as α goes to zero, so this branch doesn't exist in non-magnetic case.

When α and ϵ are small, eigenfunction are spherical harmonics and

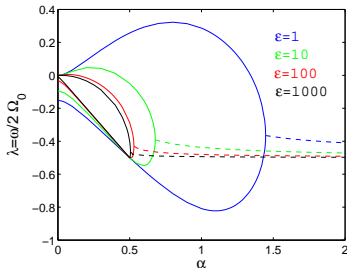
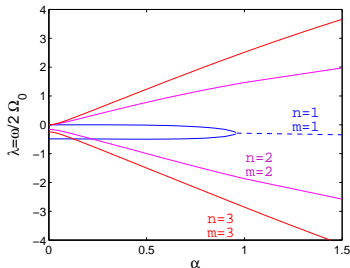
$$\omega = \frac{m v_a^2}{2 \Omega_0 R_0^2} (n(n+1) - 2),$$

so they travel eastwards. The $n = 1$ mode is anomalous, and travels very slowly westwards.

Note that magnetic Rossby waves in a full sphere travel westwards.

At large α , slow magnetic Rossby waves become polar trapped, and travel at nearly the same speed as the polar trapped fast magnetic Rossby waves, going east rather than west.

Magnetic instability when $m = 1$



When $m = 1$, the fast and slow magnetic Rossby wave branches coalesce and give rise to unstable waves. Similar behaviour in the unstratified full sphere (Malkus 1967).

Instability requires $\alpha > 0.5$. Right hand figure shows frequencies of $n = 2, m = 1$ against α for varying ϵ .

The unstable waves can be found asymptotically at large α .

Antisymmetric $B = B_0 \sin \theta \cos \theta$

This azimuthal basic state field is antisymmetric, so it is zero at the equator

The MIG waves, Kelvin waves and fast magnetic Rossby waves behave similarly to the symmetric case.

Surprisingly, slow magnetic Rossby waves are not found. Analytic studies show a singularity near the equator for these modes. Problem arises whenever the basic state field has a zero.

Need to restore magnetic diffusion to investigate the slow magnetic Rossby wave case for this field.

Summary on Shallow water MHD models

Combination of numerical and asymptotic methods result in a fairly complete picture for the simple basic state field $B = B_0 \sin \theta$.

Equatorial trapping and polar trapping can occur.

For strong magnetic fields, $\alpha > 0.5$, $m = 1$ instability can occur, though field required is too large for planetary applications.

Slow magnetic Rossby waves are more sensitive to the exact field configuration, and more work is needed here. Some features of the geomagnetic field propagate eastward: could be connected to waves in a stably stratified layer?

Wave models in more realistic tachocline models could be investigated, in the light of the slow waves detected by McIntosh et al. 2017.